Digest Journal of Nanomaterials and Biostructures Vol. 11, No. 1, January - March 2016, p. 313 - 319

SYNTHESIS AND LUMINESCENE PROPERTIES OF Sr_2CeO_4: Eu^{3+}, Tb^{3+} PHOSPHORS

Q. LI*, Z.P. LIU, X. J. LI, L. M. DONG
College of Materials Science and Engineering, Harbin University of Science and Technology, Harbin, China

A series of Sr_2CeO_4: Eu^{3+}, Tb^{3+} phosphors were prepared via sol-gel method. The X-ray diffraction（XRD）, scanning electron microscopy (SEM), TG-DTA and fluorescence spectrophotometer were exploited to characterize the samples. The obtained phosphors can be effciently excited in the range from 450 to 470 nm, Under 465 excitation, the Sr_2CeO_4: Eu^{3+} phosphors emit intense red light at 614nm, which is attributed to Eu^{3+} $^5D_0$-$^7F_2$. The doping with a suitable amount Tb^{3+} can improve the luminescence properties. As charge compensator, Li^+, Na^+, K^+ can improve the luminous intensity of the sample, among which, the effect of Li^+ is obvious.

(Received January 19, 2016; Accepted March 31, 2016)

Keywords: Cerium strontium phosphor, Rare earth ions, Sol - gel method

1. Introduction

In recent years, the synthesis and spectroscopic properties of luminescent materials containing rare earth ions has gained much attention in the fields of fluorescent lamps, Light emitting diodes (LEDs), Field emission displays (FEDs), Plasma display panels (PDPs) and high energy detectors[1-3]. Among these applications phosphor are important candidates for solid state lighting in converting white light emitting diodes (pc - WLEDs) because of their excellent properties, such as long operational lifetime, energy saving, high brightness, higher luminescent efficiency, compactness, and environment friendliness [4,5].Their exceptional electronic and optical properties result from the properties of the 4f shell of these ions,[6-11] where the structure of Eu^{3+} is $4f^6$. Fluorescence properties are more lively, excited state lifetime is long enough and it could transmit good monochromaticity, high quantum efficiency of red fluorescence, which is widely used in light-emitting material activator.

Currently there is only one tetravalent cerium ions luminescence, which is Sr_2CeO_4. Sr_2CeO_4 can be used as an excellent luminescent substrate material because of its broad excitation and emission and strong absorption of blue light. Meanwhile, Sr_2CeO_4 phosphor also has a special one-dimensional chain structure, the distance between one chain and another is only 0.3597nm, resulting in the energy transfer between activators and Sr_2CeO_4 becomes very easy, which has great help on developing new luminous materials. Under blue light excited, Sr_2CeO_4 emit a high efficiency red light because of its unique structure.

At present, Sr_2CeO_4 were synthesized by many methods and its luminescence mechanism

*Corresponding author: qinalily@163.com

and in photoluminescence, electroluminescence, cathode ray display and solar energy conversion film and other aspects of nature were studied [12-19]. In this study, Sr_2CeO_4: Eu^{3+}, Tb^{3+} light emitting material were prepared by using sol-gel method, and the luminescene properties were characterized.

2. Materials and methods

2.1. Materials Preparation

All of the chemical reagents used in this experiment were analytical grade. According to a certain proportion weighed amount, the $Sr(NO_3)_2$ and $Ce(NO_3)_3$ were dissolved in an appropriate amount of distilled water, and the $Eu(NO_3)_3$ solution was obtained after dissolving Eu_2O_3 in an appropriate amount of nitric acid, then the above solutions were mixed. Citric acid was slowly added to the mixing solutions, after which the amount of ethanol and polyethylene glycol was added to the solution. The resulting mixture was placed in a water bath at 80^{o}C, a yellow gel was obtained, and then it was placed in 80 ^{o}C oven for drying, after drying the porous fluffy dry gel was obtained. The sample was placed in a crucible and calcined in high-temperature resistance furnace at a temperature to obtain Sr_2CeO_4 phosphor powder.

2.2. Analysis Methods

The structures of the phosphor were established by X-ray diffractometer (XRD) (Shimadzu, XRD-6000, Cu Ka target) and the morphology of the particles was observed by field emission scanning electron microscope (FE-SEM) (Sirion 200, Philip). The photoluminescence properties of the phosphors were studied on fluorescence spectrophotometer (Shimadzu, model RF-5301 PC). All the photoluminescence properties of the phosphors were measured at room temperature.

3. Results and discussion

3.1 Phase Identification and Crystal Structure.

The phase composition and purity of the as-prepared powder samples were detected by XRD. Figure 1 shows the representative XRD patterns for Sr_2CeO_4:0.08Eu^{3+}, 0.01Tb^{3+}samples. It shows that all the diffraction peaks match well with that of standard JCPDS card (No. 50−115); and no other phase of the peak were detected, indicating the prepared samples were single phase. According to the XRD patterns, we can deduce that the $Eu^{3+}$and Tb^{3+} ions were completely dissolved in the Sr_2CeO_4 host without inducing significant changes of the crystal structure. The Sr_2CeO_4 crystallizes in the orthorhombic space group Pbam with cell parameters of a = 6.118Å, b = 10.349Å, c =3.597Å.

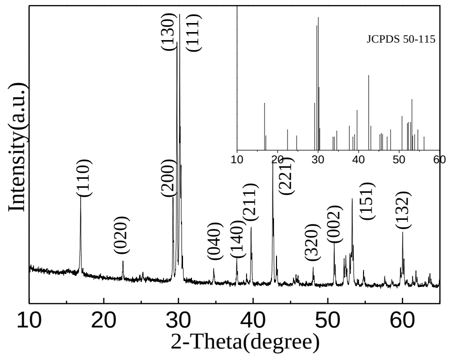

Fig. 1: Representative XRD patterns of Eu^{3+} and Tb^{3+} doped Sr_2CeO_4 samples synthesized at 1000°C for 4h. The reference is standard card data of Sr_2CeO_4 (JCPDS Card No. 50−115) is shown as a reference.

3.2 Thermal Analysis

The precursor solution was evaporated to yield gel powder, which was analyzed by TG-DTA. Figure 2 illustrates TG/DTA of Sr_2CeO_4: Eu^{3+}, Tb^{3+} precursor. The TG curve showed two steps in this measurement and weight loss finished around 1000 °C。Endothermic peaks appeared at around 203, 282, and 408 °C and exothermic peaks also appeared at 486 and 798 °C. These peaks correspond to the decomposition of nitrate at high temperatures, there are endothermic peak on the DTA curve corresponding to endothermic peaks (first two peaks), decomposition of Citrate(408 °C and 486 °C), and the last peak at 798 °C might correspond to the decomposition of $SrCO_3$ and formation of Sr_2CeO_4. On the basis of the result from the TG-DTA analysis, the cerats particles prepared were calcined at 1000 °C.

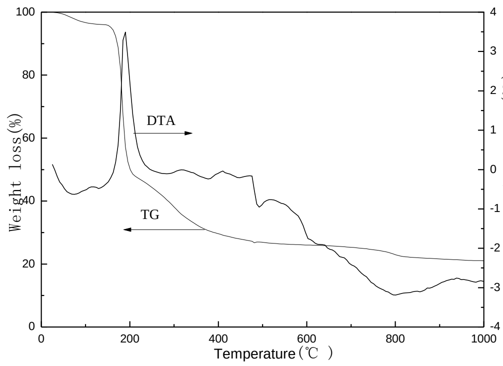

Fig. 2: TG-DTA curves of Sr_2CeO_4: Eu^{3+}, Tb^{3+} gel powder.

3.3 SEM Images

The morphologies of the final samples were investigated by SEM. Figure 3 presents the SEM images of Tb^{3+} un-doped samples and Tb^{3+} doped sample, respectively. What we can see in the picture is that the samples with Tb^{3+} doped shows smaller particles and more uniform size(Figure 3b).

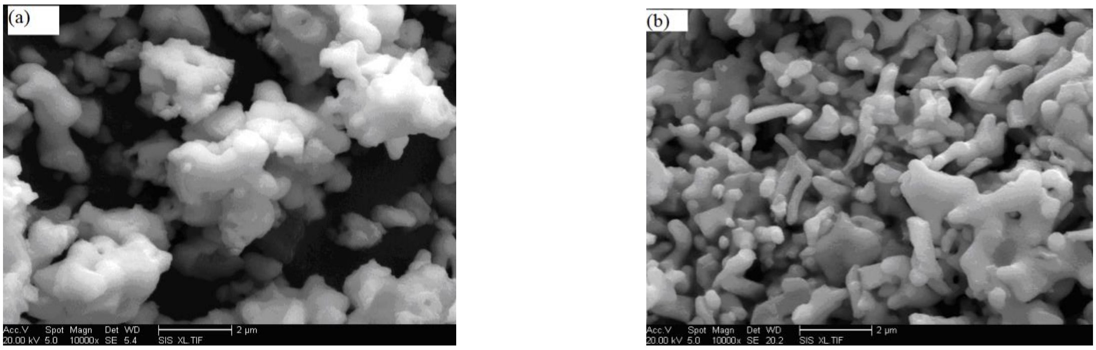

Fig. 3:. SEM images of Tb^{3+} undoped samples (a) and Tb^{3+} doped sample (b) firing at 1000 ^{o}C

Tb^{3+} un-doped sample shows larger particles and irregular shape, which may be due to that the surface energy distribution of sample is uneven, resulting in abnormal growth of crystals in certain crystal, leading to the agglomerate of particle.

3.4 Luminescence properties of Eu^{3+} doped materials

Fig. 4 depicts the photoluminescence (PL) and photoluminescence excitation (PLE) spectra of the as-prepared Sr_2CeO_4: $0.1Eu^{3+}$ phosphor. In the excitation spectrum (Figure 3, left)monitored at 610 nm, the sample shows a narrow weak excitation band from 385 to 400 nm and a intense band from 450 to 470 nm with a maxium at 465 nm due to the f-f transition of the Eu^{3+} ions. Upon excitation at 465 nm, the emission spectrum (Figure 3, right) of Sr_2CeO_4: $0.1Eu^{3+}$ sample consists of the characteristic transition lines between Eu^{3+} levels. The emission spectrum exhibits three groups of emission lines at 538, 593 and 616nm, which are assigned to the $^5D_1$-$^7F_1$ and $^5D_0$-^7F_J(J = 1, 2) transitions of Eu^{3+}, respectively. Obviously, the emission spectrum is dominated by the red $^5D_0$-$^7F_2$(610 nm) transition of the Eu^{3+}, which is an electric-dipole-allowed transition and hypersensitive to the environment.

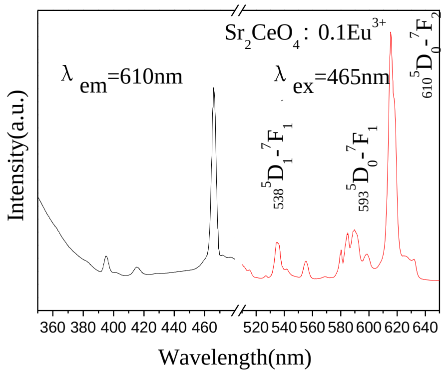

Fig. 4: PL and PLE spectra of Sr_2CeO_4: $0.1Eu^{3+}$ phosphor

In order to investigate the effect of doping concentration on luminescence properties, a series of Sr_2CeO_4:mEu^{3+}(m=0.01,0.05, 0.08, 0.10, 0.15) phosphors were synthesized. Figure 5 shows the PL spectra of Sr_2CeO_4: mEu^{3+} with different doping contents. The red emission of the Eu^{3+} increases gradually and reaches a maximum at m = 0.10. With further increment of Eu^{3+}

concentration, the emission intensity begins to decrease due to concentration quenching. According to the Dexter's energy transfer theory[20],concentration quenching is mainly caused by the nonradiative energy migration among the Eu^{3+}ions at the high concentration.

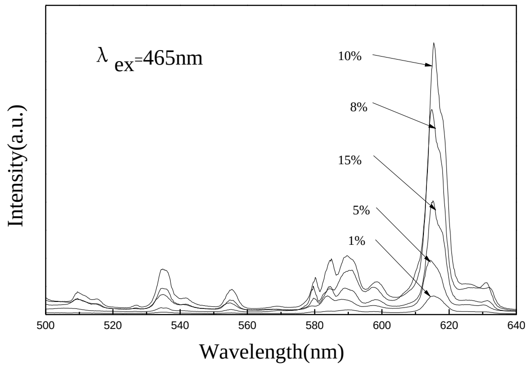

Fig. 5: Emission spectra for Sr_2CeO_4: mEu^{3+} with various doped Eu^{3+}molar concentration (m).

3.5 Luminescence Properties of Sr_2CeO_4:Eu^{3+}, Tb^{3+} Phosphor

A series of phosphors with fixed $Eu^{3+}$and Tb^{3+}content were prepared to study the effect of doping concentration on the luminescence properties of phosphors. Figure 6 shows the PL spectra of the Sr_2CeO_4:0.1 Eu^{3+}, nTb^{3+} phosphors with n varying from 0 to 0.012.When the Eu^{3+} doped concentration is high, the phosphor has a strong emission at 616nm.There was no effect on the shape of the emission spectrum with the doping of Tb^{3+}.

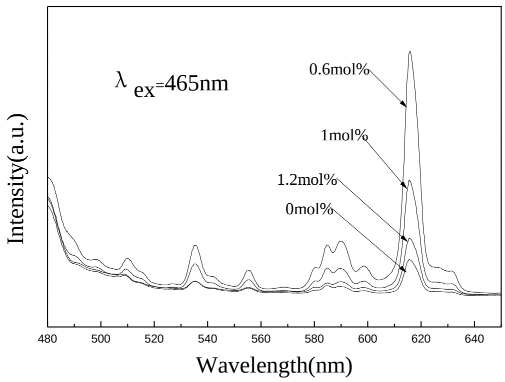

Fig. 6: PL spectra of Sr_2CeO_4:0.1 Eu^{3+}, Tb^{3+} phosphors with variousTb^{3+} content

The intensity of emission spectrum enhance with the increasing of Tb^{3+}content. Since the concentration increases to a certain value, the intensity of emission spectra is the strongest. With the increasing of Tb^{3+}content, the intensity of emission spectra reduces. The doping of a suitable amount of Tb^{3+} will improve the luminescence properties of the luminescent material.

3.6 The Effect of Charge Compensation

Fig. 7 shows the PL spectra of Sr_2CeO_4: Eu^{3+}, Tb^{3+} phosphor with Li^+, Na^+, K^+ doping. Eu^{3+} ions replace the matrix Sr^{2+} ions, creating a negative charge in the lattice. Thus, Li^+, Na^+, K^+ as charge compensator was considered to introduce. There are lattice distortion when the introduction of Li^+, Na^+, K^+, which has a positive on the transition of Eu^{3+}, thus improving the luminous intensity. As can be seen from figure 7, different charge compensation has different impact on improving the fluorescence intensity, which can be explained by the different sizes of compensator. As we all know, the radius of Sr^{2+} is 0.118nm, and 0.059nm, 0.116nm, 0.133nm of Li^+, Na^+, K^+, respectively. Compared with Na^+ and K^+, the radius of Li^+ is smallest, leading to that Li^+ has more chances to enter the host lattice.

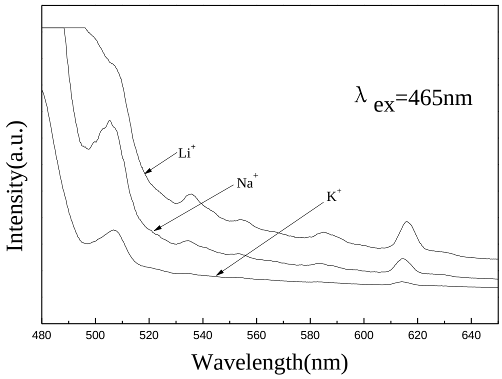

Fig.7: PL spectra for Doping Li^+, Na^+, K^+ as the charge compensation agent of Sr_2CeO_4: Eu^{3+}, Tb^{3+} phosphors

4. Conclusion

In summary, a red-emitting phosphor Sr_2CeO_4: Eu^{3+}, Tb^{3+} was synthesized by the sol-gel method, the photoluminescence properties and crystal structure were investigated. The Sr_2CeO_4 host has an orthorhombic unit cell with cell parameters a = 6.118Å, b = 10.349Å, c =3.597Å. The obtained phosphors have a narrow excitation band ranging from 450 to 470 nm. At the excitation of 465 nm, the Sr_2CeO_4: Eu^{3+} phosphors can emit intense red light with an optimal concentration of the Eu^{3+} being 0.1. For the co-doped samples, Tb^{3+} doped with a suitable amount can improve Sr_2CeO_4: Eu^{3+}, Tb^{3+} luminescence properties of the luminescent material. Charge compensator Li^+, Na^+, K^+ can improve the luminous intensity of the sample, among which, the effect of Li^+ is obvious.

References

[1] C. Guo, H. Jing, T. Li, RSC Adv. **2**, 2119 (2012).
[2] M. Xie, C. Luo, Phys. Status Solidi (RRL) **6**, 412 (2012).
[3] I. Valais, C. Michail, S. David, et al., Phys. Med. **24**,122 (2008).
[4] C.C. Lin, R.S. Liu, J. Phys. Chem. Lett. **2**, 1268(2011).
[5] S. Ye, F. Xiao, Y.X. Pan, et al., Mater. Sci. Eng. R. **71**,1(2010).
[6] Binnemans, K. Chem. Rev., **109**, 4283 (2009).
[7] C. Görller-Warland, K.Binnemans, In Handbook on the Physicsand Chemistry of Rare Earths; Gschneidner, K. A., Eyring, L., Eds.; North Holland: Amsterdam,; **25**, 101 (1998).
[8] G.Liu, B.Jacquier, Spectroscopic Properties of Rare Earths in Optical Materials; Springer:

New York, **83**, 25 (2005).
[9] C. Jørgensen, R. Reisfeld, New Trends Chem., **100**, 127 (1982).
[10] Bünzli, J.-C. G. Acc. Chem. Res., **39**, 53(2006).
[11] J.-C. G.Bünzli, C.Piguet, Chem. Soc. Rev., **34**, 1048 (2005).
[12] L. Pieterson, S. Soverna, A. Meijerink, J Electrochem Soc., **147**(12), 4688(2000).
[13] C. H. Park, C. H. Kim, C. H. Pyum, et al., J Lumin, **87-89**, 1062 (2000).
[14] Y. E. Lee, D. P. Norton, J. D. Budai, Appl Phys Lett , , **77**, 678 (2000).
[15] Y. X. Tang, H. P. Guo, Q. Z. Qin, Solid State Commun , **121**, 351 (2002).
[16] Jiang Y D, Zhang F, Chriatopher J, et al., Appl Phys Lett, **,74**, 1677 (1999).
[17] X. M. Liu, Y. Luo, J. Lin, J Crystal Growth, **290**,266 (2006).
[18] N.Perea, G.A. Hirata. Optical Mater., **27**, 1212 (2005).
[19] N. Perea, G. A. Hirata, Thin Solid Films, **497**, 177 (2006).
[20] D. L. Dexter, J.Chem Phys, **22**(5),1063 (1954)